KU LEUVEN

TECHNISCHE UNIVERSITÄT DRESDEN

Tuning Threshold Voltage in Organic Electrochemical Transistors by Varying Doping of the conjugated polymer p(g3T2-T)

Marielena Velasco Enriquez

Academic year 2022 – 2023

Preface

Marielena Velasco Enriquez

Contents

Abstract

Organic Electrochemical transistors (OECTs) exhibit advantageous properties, such as high transconductance and steep-slope switching, while operating at very low voltages. Although, their switching speed is comparatively slower than solid-state devices, it remains sufficient for applications in bioelectronics [1]. The gold standard semiconductor for p-type OECTs is PEDOT:PSS. However, its main drawback lies in its depletion-mode operation, which requires power to turn off the device. To minimize power consumption and improve stability, efforts have been made to the design conjugated polymers that allow accumulation-mode devices. One such polymer, 3-(2-(2-(2-methoxyethoxy)ethoxy)ethoxy)thiophene (p(g3T2-T)) has demonstrated negative threshold voltages close to zero and high transconductance [2]. Furthermore, by doping p(g3T2-T) at various levels and drop-casting it as a gate, it has been possible to fine-tune the threshold voltage [3]. This study aims to adapt a microstructuring method for fabricating side-gated OECT devices that comprises different doping levels of F_4TCNQ and F_6TCNNQ in p(g3T2-T) and a solid-state electrolyte [4], the latter is deposited by inkjet printing. Additionally, the study aims to adjust the threshold voltage by utilizing these varying doping levels, while analyzing the stability and performance of the doped devices.

List of Figures and Tables

List of Figures

List of Tables

Chapter 1

Introduction

The field of organic electronics has witnessed significant advancements in recent years due to its biocompatibility, mechanical compliant, and other application-specific characteristics. Among the numerous types of organic devices, Organic Electrochemical Transistors (OECTs) have attracted considerable attention due to their unique capabilities such as high transconductance and steep-slope switching at low operation voltages, which give them potential for use in energy storage, bioelectronics and neuromorphic devices.

Accumulation-mode transistors, devices that are normally in the OFF state at zero-gate-biased condition, rely on the use of undoped conjugated polymers. In contrast, the ability to precisely control and tune threshold voltage of an OECT can be achieve by manipulating the doping level of the mentioned conjugated polymer [3]. Tan et al. fabricated devices that did not follow a complete microstructuring technique, limiting their integration into circuits.

The primary objective of this research is to address this missing information by developing a microstructuring method to fabricate accumulation-mode OECTs with controlled doping levels and enable their seamless integration into circuits. However, during the pursuit of this objective, it was identified that stability of dopants in an electrochemical environment may pose challenges that need to be addressed as well. Therefore, this research project specifically aims to:

1. Characterize 3-(2-(2-(2-methoxyethoxy)ethoxy)ethoxy)thiophene (p(g3T2-T)) with varying doping levels of F_4TCNQ and F_6TCNNQ. This involves chemically modifying the conjugated polymer with different concentrations of dopant and analyzing their electronic structure, morphology and electrical properties using techniques such as UV-Vis spectroscopy, Ultraviolet Photoelectron Spectroscopy (UPS), Atomic Force Microscopy (AFM), Van Der Pauw method, Electrical Impedance Spectroscopy (EIS) and Cyclic Voltammetry (CV),

2. fabricate OECT devices, which involves utilizing the conjugated polymer at different doping levels, and adapting an existing method that combines electrode patterning techniques, spin-coating, photolithography and inkjet printing. The devices will be carefully optimized to ensure reproducibility and stability,

3. assess doped polymer stability in OECT, which involves performing conductivity measurements over time and selecting an electrolyte composition that allows an stable performance, and

4. investigate the shift in threshold voltage through electrical characterization of the fabricated OECT devices with varying doping levels of F_4TCNQ and F_6TCNNQ.

The thesis is structured as follows: Chapter 1 provides an overview of organic electronics and the importance of the OECT threshold voltage, and outlines the motivation, goals, and structure of the thesis. Chapter 2 presents a comprehensive review of the relevant background information on Organic Semiconductors (OSCs), Organic Mixed Ionic Electronic Conductors (OMIECs), and Organic Electrochemical Transistors, and relevant research on tuning the threshold voltage of OECTs. Chapter 3 illustrates the Experimental Methods used in this research, describes the materials, equipment, software, and procedures to chemically doped the films and characterization method employed in the study. Finally, it outlines the fabrication and characterization process of OECT devices. In Chapter 4, the experimental results obtained are presented, from the characterization of the conjugated polymer at different doping levels and fabricated OECT devices. Analysis of the relationship between the doping level and the shift in threshold voltage. Finally, it discusses the implications of the findings and their relevance to the field. Lastly, Chapter 5 provides a summary of the research objectives and the extent to which they were achieved, suggests future research direction, and potential applications.

By addressing the aforementioned research goals and following the proposed thesis structure, this study aims to contribute in adapting an existing protocol to the conjugated material p(g3T2-T), in understanding the doping-dependent tuning of OECT threshold voltage and establish a foundation for the development of high-performance organic electronic devices.

Chapter 2

Background

2.1 Organic Semiconductors

Unlike inorganic semiconductors, organic semiconductors are lightweight, easy to chemical tune, mechanical flexible, and possess low-cost and low-temperature processing. All of these characteristics increased the attention to this type of materials in the field of organic electronics.

2.1.1 Electronic Structure

Organic semiconductors are π-conjugated molecules that comprise mostly carbon and hydrogen atoms, with alternating multiple (sp^3, sp^2 hybridization) and single (sp hybrization) bonds. This configuration exhibit p orbitals with delocalized electrons, charge transport among the length of these polymers is caused by this resonance structure. Based on the size of the conjugated system, organic semiconductors can be divided into conjugated polymers and small molecules.

2.1.1.1 Conjugated polymers

Transport properties depend on the details of the band structure, namely the density of states and the band widths

2.1.1.2 Small Molecules

Unlike conjugated polymers, the chain size of small molecules have the advantage of being ordered and its synthesis allow to obtain high purity material.

2.1.2 Molecular Doping

The basic principles are similar than in inorganic materials, "where electron donors or acceptors are added and generate additional mobile charge carriers", as shown in Figure 4.1. While n-type dopants donate electrons to the lowest unoccupied molecular orbital (LUMO) states, the "p-type dopants extract electrons from the highest occupied molecular orbital (HOMO) states", hence creates holes [5]. In
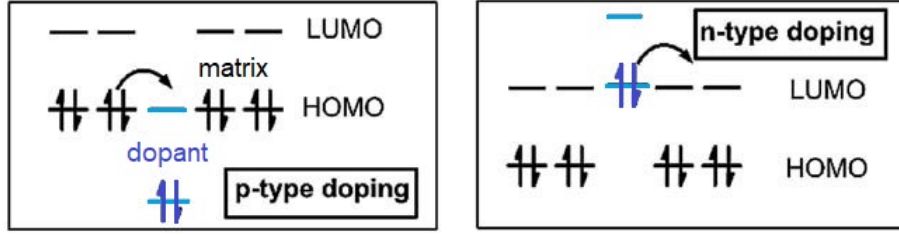
FIGURE 2.1: Schemes for p-type (left) and n-type (right) doping processes. Extracted from reference [5].

other words, the Fermi level E_F of the polymer will shift towards the LUMO (or HOMO) level when n-type (or p-type) doping. Shift that can be measured by spectroscopy techniques such as Ultraviolet Photoelectron Spectroscopy (UPS) at room temperature (RT) [9], limited to the penetration depth of the incoming electron.

The use of small molecules is commonly reported as dopants for organic materials. Some strong acceptor (or electron-defficient) molecules that are widely used are 2,3,5,6 tetrafluoro-7,7,8,8-tetracyanoquinodimethane (F_4TCNQ) or 1,3,4,5,7,8 hexafluoro-7,7,8,8-tetracyanonaphthoquinodimethane (F_6TCNQ), which also take part in this work. The latter exhibits a higher electronic affinity (-5.3 eV) or deep HOMO than F_4TCNQ (-5.2eV) meaning that it can abstract more electrons, specially to polymers with low ionization potential (less than 5eV) or shallow LUMO, [8], as it is the case of p(g3T2-T) acting as donor.

Among the different methods to molecular doped a conjugated polymer, Jacobs et al. compared a solution-mixed and solution sequential doping of P3HT (a thiophene-based polymer) doped with F_4TCNQ, both straightforward and easy methods for doping [10]. In this work it was demonstrated that solution-mixed films are considerably rougher than solution-sequential films, affecting negatively to its conductivity. The fact that solution-sequential doped films allows better homogeneity, make it also more compatible with microstructuring processes such as photolithography. At the expense of having less control over the doping levels compared to solution-mixed films [11].

2.2 Organic Mixed Ionic/Electronic Conductors (OMIECs)

Organic Mixed Ionic/Electronic conductors are organic semiconductors that allow the conduction of electrons (or holes) and ions, the latter set them apart from other organic semiconductors.

Initially investigated for batteries and super capacitors [12] [13], where the induction of charges in a semiconducting polymer was the main objective. OMIECs has rapidly grown to include other applications, among them, our focus: OECTs.

Paulsen et al. classified OMIECs into six different categories according to whether they *"intrinsically contain ionic charge"* (I, III, V) or not (II, IV, VI), the latter
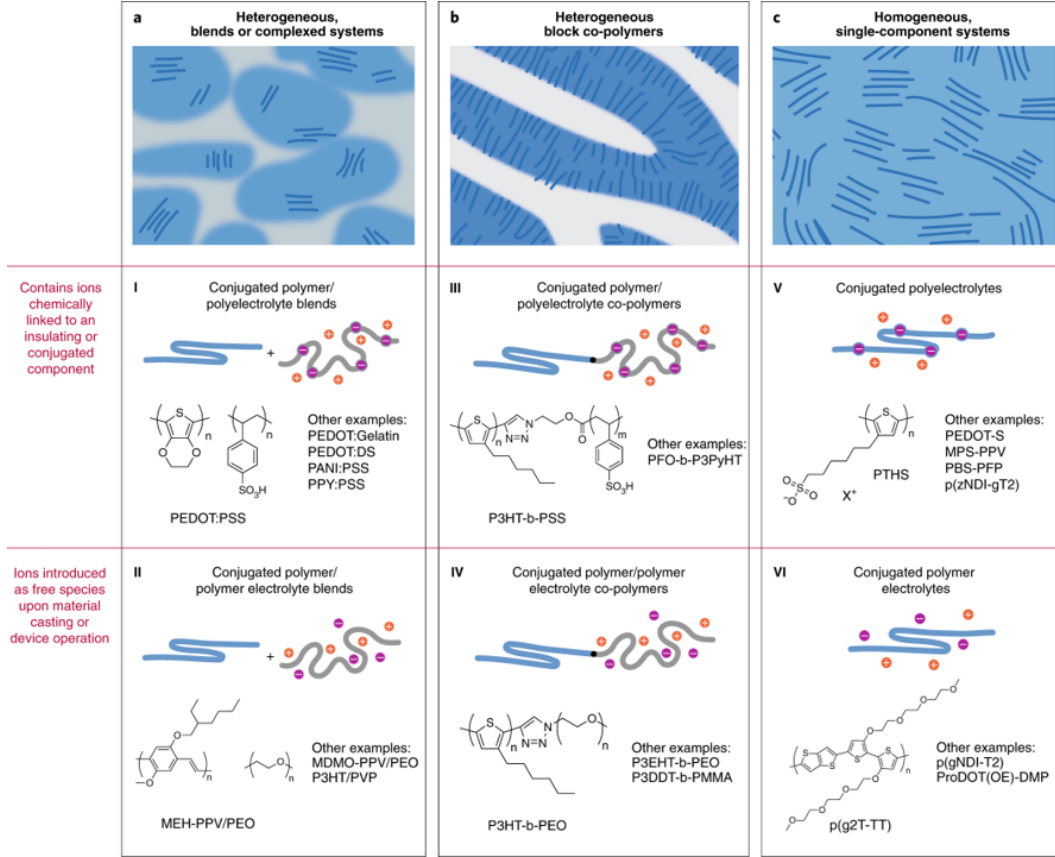
FIGURE 2.2: **Material classes of OMIECs.** a) Heterogeneous blends of an electronically conducting conjugated polymer with (I) an ionic charge bearing polyelectrolyte or (II) an ion solvating polymer electrolyte. b) Heterogeneous block copolymers of an electronically conducting conjugated polymer with (III) an ionic charge bearing polyelectrolyte or (IV) an ion solvating polymer electrolyte. c) Fully conjugated (V) ionic charge bearing polyelectrolytes and (VI) ion solvating polymer electrolytes. Extracted from reference [6].

"contain polar moieties that can solvate ions". Another distinction among the categories is whether the conjugated system comprises a single material (homogeneous, type V and VII) or two-component, more complex systems or block co-polymers materials (heterogeneous, type I, II, III, IV)[6], an schematic representation is shown in Figure 2.2.

2.2.1 Processes in OMIECs

2.2.1.1 Ionic-electronic interactions

The presence of electronic charge in OMIECs requires also the presence of excess ionic charge, so charge in the system remain balance. In the case of types II, IV and VI OMIECs, the so-called stabilizing electrochemical doping is achieved by the

presence of mobile ions, the remaining type of OMIEC on the other hand, have this stabilizing charges fixed, they are inherently doped.

The amount of coupling between electronic charge and excess ionic charge in OMIECs can be modulated with an applied bias when coupled through an electrolyte [6]. This is the basic principle of OECTs, and we will be further discuss in section 2.2.2.

2.2.1.2   Electronic transport

Electronic charge carrier density in undoped semiconductor organic species is logically low (no accessible hopping states), but in contact with an electrolyte, due to the ionic-electronic coupling as described in previous section, dopant ions would lower the activation energy of charge hopping and increase carrier mobility [6]. Electronic charge transport mechanisms, that can be within the length of the conjugated polymer (thermally activated hopping) or within the polymer-stacking (band-like transport) are represented in Figure 2.3.

(A)   (B)
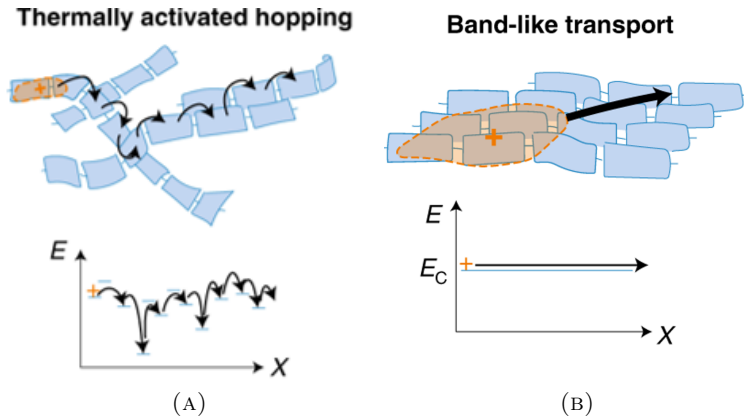
FIGURE 2.3: Schematic representation of electronic charge transport mechanisms: A) "Thermally activated hopping transport of a relatively localized electronic charge carrier" and B) "band-like transport of a relatively delocalized electronic charge carrier". Modified from reference [6].

2.2.1.3   Ionic transport

Although transport of charged anions and cations can be seen analogous to electrons and holes, they remain more complex, since they can be *"multi-valent, and form pairs and larger clusters; morever, they are sensitive to solvent and solvation"* [6].

Ion transport for dry OMIECs of type I, III and V are unipolar since they are fixed on a polyelectrolyte. However, when they are in contact with an electrolyte, swelling occurs, which allows the penetration of excess ions from the electrolyte, therefore both mobile anions and cations would contribute to ion transport.

Then two types of ionic charge transport can be differentiated: ion hopping and solvated ion vehicle transport, as described in Figure 2.4a and b, respectively. In dry or minimally hydrated OMIECs only ion hopping occurs, whereas when OMIEC is in contact with solvent or liquid electrolyte, both mechanisms occur. The latter basically explains how ionic transport in OECTs (and other OMIEC-electrolyte based applications) is rather complex and needs to consider all ionic-electronic coupling, hydration and electrolyte swelling [6], which will be further discuss in section 2.2.2.
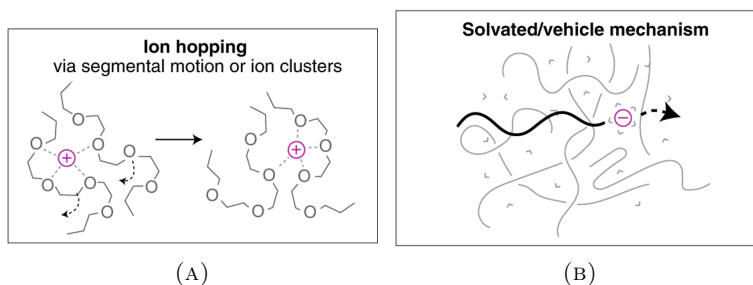
FIGURE 2.4: Schematic representation of ionic charge transport mechanisms: A) "Segmental motion-assisted ion hopping" and B) "solvated ion vehicle transport". Modified from reference [6].

2.2.2 Electrochemical Doping

"The electrochemical charging of OMIECs can be described as a capacitive faradaic charging process, meaning that the OMIEC" is p-doped (oxidized, in the language of chemists) "through an electron transfer with the contact (current collector), while ions from the electrolyte penetrate inside the channel material to compensate the charge carriers on the polymer backbone electrostatically with no change in the inserted ion's oxidation state" [14]

2.3 Organic Electrochemical Transistors (OECTs)

Organic Electrochemical Transistors (OECTs) consists of metallic source, drain and gate electrodes, an organic conjugated polymer channel (specifically an OMIEC as described in previous sections) and an electrolyte that couples channel and gate. Devices that have received increasingly attention due to their mechanically compliance, biocompatibility, and are sensitive to biochemical modules [15].

2.3.1 Device Physics

Although the structure of OECTs are different from conventional metal-oxide-semiconductor field-effect transistors (MOSFETs). The basic understanding of the latter can give us a clear idea of how OECTs operate. Unlike MOSFETs, OECTs are coupled with an electrolyte rather than an insulator. So, when applying a
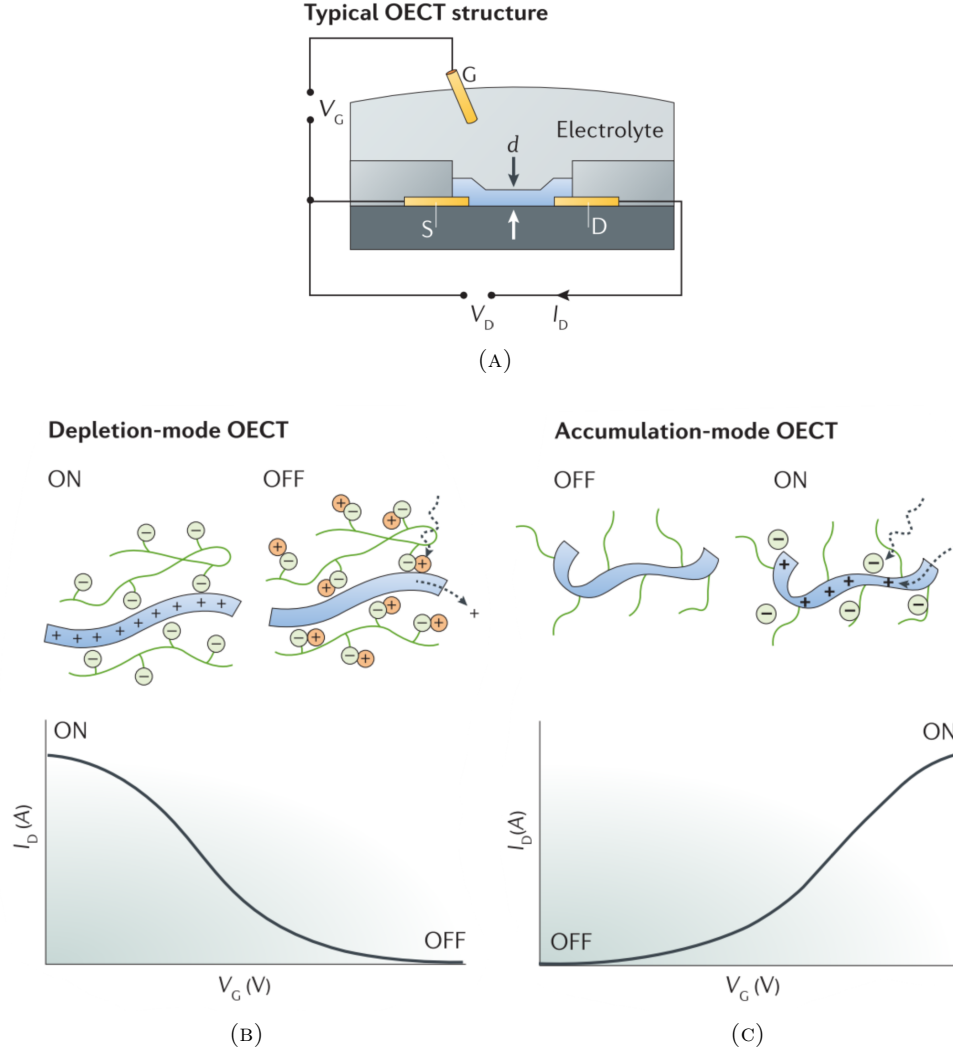
FIGURE 2.5: (A) Typical structure of an organic electrochemical transistor (OECT). (B) Transfer curve showing depletion-mode operation of an OECT with a conducting polymer channel. (C) Transfer curve showing accumulation-mode operation of an OECT with a semiconducting polymer channel. Images extracted from reference [1].

gate voltage, instead of polarizing the dipoles in the insulator, creating a field that causes accumulation of carriers at the interface of the semiconductor/insulator as happens in a MOSFET, the gate voltage would rather drive ions to penetrate the bulk of the channel, so accumulation of carriers will happen throughout the whole volume of the OMIEC film. This explains the large gate-channel capacitance in these devices compared to MOSFETs, and why drain-source current takes into account a volumetric capacitance [16].

Bernard et al. implemented a model based on a p-type depletion-mode OECT (since PEDOT:PSS is widely fabricated and investigated, further discussed in the
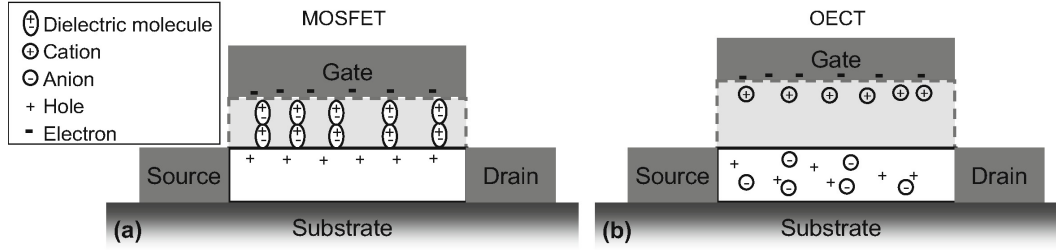
FIGURE 2.6: Comparison of p-type A) MOSFET and B) OECT. Where the light-gray region represents an insulator and a electrolyte, respectively.

following section). The model divides the behavior of the OECT into an electronic and an ionic circuit. The electronic circuit is modeled using Ohm's law and upon the application of a positive gate voltage, in a p-type OECT, de-doping of the semiconductor occurs, analogous to the compensation doping of Silicon, cations from the electrolyte penetrate the polymer, compensating one acceptor. [7]
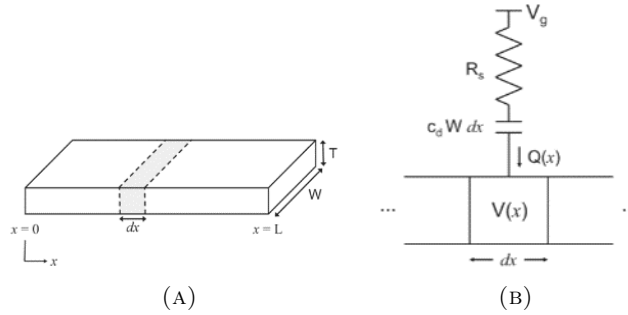
FIGURE 2.7: Representation of device model, A) OMIEC film with source and drain located at x=0 and x=L, respectively, B) Ionic circuit charge (Q) is coupled to the voltage in the electronic circuit. Image extracted from reference [7].

2.3.2 Operation Modes

As seen in Figure 2.5B) and C), the OMIEC can be conductive (such as PEDOT:PSS) or semiconducting (such as p(g3T2-T). Both will describe a normally ON and OFF device, respectively at zero-gate biased.

Due to its commercial availability, operational stability, and relatively high performance, PEDOT:PSS became a standard material for p-type OECTs. Its main drawback lays in its depletion-mode operation, which requires a voltage to turn off the device (as represented in Figure 1(b)). With the aim of minimizing power consumption, there is a special interest to design semiconducting polymers that would allow accumulation-mode devices (Figure 1(c)) with high performance [2] [11].

Accumulation-mode devices has the advantage of dissipating less static power when the device is not operated, due to low OFF current, which must be minimized

9

as much as possible [14]

Nielsen et al. reported a series of semiconducting polymers with Ethylene Glycol (EG) side chains designed to elucidate important strcuture-property guidelines for accumulation-mode OECT operation. They demonstrated that an OECT with 3-(2-(2-(2-methoxyethoxy)ethoxy)ethoxy)thiophene p(g3T2-T), as seen in Figure , has higher transconductance, and a turn-on voltage close to zero compared to other thiophene-based species [2]. While its backbone design warrant reversibility during electrochemical redox reactions and good electronic transport, the EG side chains enable its stability in aqueous electrolytes and efficient transport of ionic and electronic charge carrier [17]. Moser et al. studied the impact of the length of the EG side chain of this polythiophene backbone on the performance of OECTs. They reported that reducing chain length would maximize the capacitance, but the increase of length would enhance ion-polymer interaction. Finally, they suggested an optimum length of 3 monomers in side chains over 2, 4 and 6 monomers [18]. The main advantage of p(g3T2-T) over PEDOT:PSS is its higher transconductance [2], the absence of extensive pre- and postprocessing to optimize polymer stability and electrochemical performance in aqueous media and the possibility of an accumulation-mode OECT with low operation voltages[18].

2.3.2.1   A widely used material: PEDOT:PSS

"Prototypical semiconductor used in OECTs ... doped with ..., is a degenerately doped p-type semiconductor (commonly referred as to as a conducting polymer)" [7]

Poly(3,4-ethylenedioxythiophene) poly(styrene-sulfonate) (PEDOT:PSS) is an organic conducting polymer that is widely used in multiple applications in organic electronics. Classified as type I OMIEC according to Figure 2.2, it is a blend between a conjugated polymer (PEDOT) and a polyelectrolyte (PSS), the latter posses chemically linked ions and serves as a polymeric acid template to allow dispersable suspensions.

2.3.2.2   Other Thiophene-based polymers

Thiophene is a planar conjugated ring structure consists of six delocalized pi-electrons. The aromatic nature arises from the four pi electrons and one unshared lone pair of electrons of the oxygen as six delocalized pi-electrons. It folow Hucke´s rule. Hence it is aromatic compound.

Organic semiconductors with polar sidechains have been identified as a promising class of materials for the field of bioelectronics. These materials, also called organic mixed ionic/electronic conductors (OMIECs), can exchange ions with aqueous electrolytes when electronic charge carriers are injected, transported, and stored in the bulk of the material [14]

Under the classification shown in Figure 2.2, p(g3T2-T) can be identified as a type VI OMIEC that comprises a conjugated polymer with ions introduced as **free species** wheareas PEDOT:PSS' ions are **chemically linked** to the polyelectrode (PSS) and blended to the conjugated polymer (PEDOT). This structural characteristic make
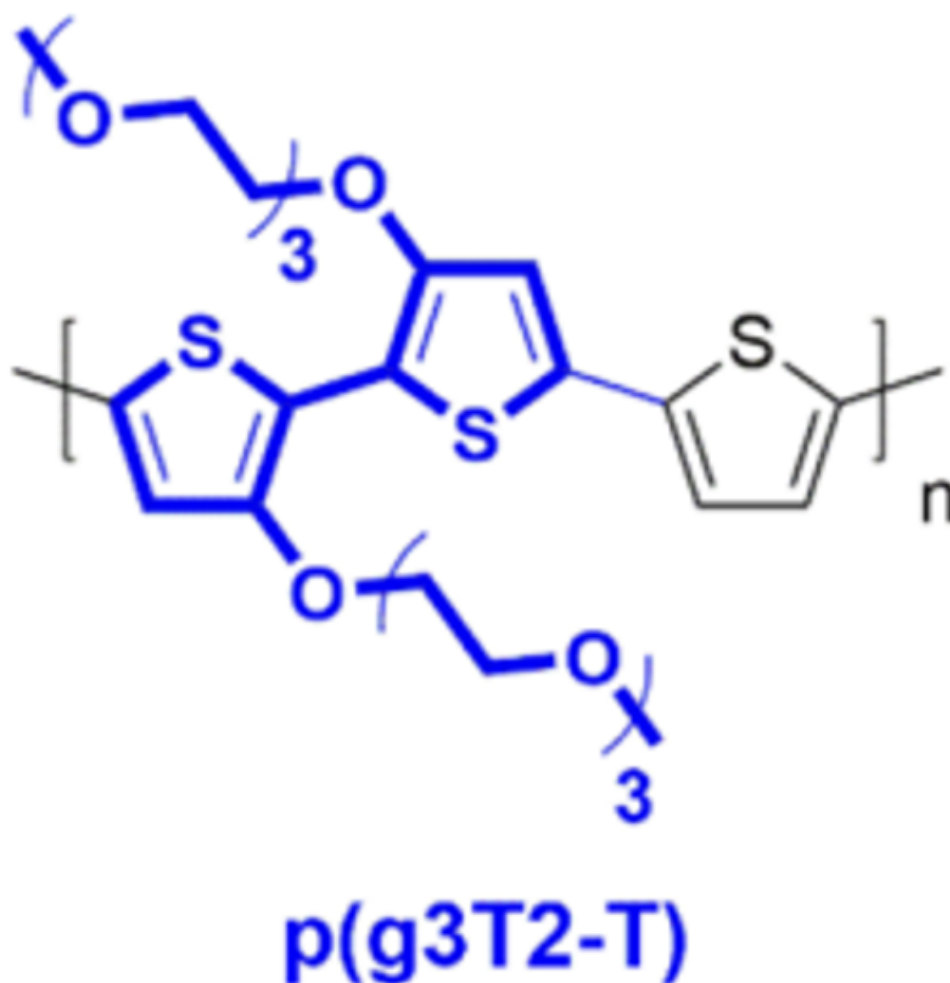
FIGURE 2.8: pg3t

p(g3T2-T) display larger magnitudes of ionic-electronic coupling but at the same time will be important for understanding the challenges on having a stable OECT with our material and will be bring back in Section 2.3.3.3.

The modulation of the degreee of electrochemical doping in OECTs with an applied biased, will manifest a potential-dependent capacitance (C). Homogeneous single phase OMIECs (type V and VI) display larger magnitudes of ionic-electronic coupling and larger values of volumetric capacitance than biphasic OMIECs such as PEDOT:PSS [19]

2.3.3 Important Figures of Merit

2.3.3.1 Transconductance

2.3.3.2 μC* product

2.3.3.3 Threshold voltage

An approach to shift the operating voltage range for PEDOT:PSS OECTs to lower the channel current, leading to reduced power consumption, is to tune the threshold voltage by de-doping PEDOT:PSS using commercially available amine-based molecular de-dopants [20]. Tan et al., on the other hand, explored a different approach, rather than modifying the doping level of the channel, they tuned the doping level of the gate to shift the threshold voltage. They used p(g3T2-T) and obtained a 400mV change with 60% mol ratio of 2,3,5,6-Tetrafluoro-7,7,8,8-tetracyanoquinodimethane (F4TCNQ) dopant. The advantage over this approach is i) protecting the material from oxidation, since the Fermi level in brought towards the highest occupied molecular orbital (HOMO), and ii) no interference with the channel which helps to leave the transconductance unaffected [3].

2.3.4 Requirements to Avoid Undesirable Side Reactions

Achieving effective charge transfer between the analyte and OMIEC requires appropriate alignment of the electrochemical potential of electrons on the OMIEC electrode and the redox specie. Failure to do so may result in the subsequent transfer of charges to other redox-active sinks in the environment, leading to undesirable side reactions and products that may interfere with the OMIEC's operation. Electrons flow from a region of higher to lower electrochemical potential. Hence, achieving electron transfer from redox-active species to the OMIEC requires the latter to have a deep LUMO (high electron affinity) [15]

Capacitive fading upon cycling

2.3.4.1 Water uptake

Savva et al. study the influence of water on the performance of OECT, the water uptake of conjugated polymer films led to 10-13% mass increase under non biased conditions. As the concentration of water decrease (NaCl$_{aq}$ 10 mM, 100mM, 1M, and 6M) ionic charging is faster regardless of the doping pulse, however the fastest ionic charging is achieved at NaCl$_{aq}$ 1 M. The injection/drift of ions is also affected by the ion-counterion attractive forces which delays the ion injection from the electrolyte, opposing their drift into the polymer (NaCl$_{aq}$ 6 M hinders the drift of anions) affecting the response time. [21]

2.3.4.2 Oxygen Reduction Reaction (ORR)

With the aim of developing accumulation-mode OECTs, the engineering of new OMIECs were introduced as commented in previous sections. Normally, this polymer backbones have low ionization potential (IPs) which lead to another side effect issue

that little attention has been paid: non capacitive faradaic rections in ambient: electron-transfer reaction from the OMIEC to molecular oxygen described as oxygen reduction reaction (ORR)

The ORR yields either H_2O_2 or water (H_2O) as well as charging (oxidation) of the OMIEC that acts as the catalyst. The first shows a free energy difference that is endergonic for OMIECs with IPs 4.9eV and hence prevent the OMIEC from undergoing ORR that form H_2O_2. To prevent the ORR in ambient conditions, OMIECs based on donor-acceptor copolymer (Type III or IV) that have large IPs to shift [14]

2.3.5 Building Block for neuromorphic and bioelectronic applications

Chapter 3

Experimental Methods

3.1 Materials

All reactives were purchased from commercial suppliers and non further chemical modification or purification was done unless stated before.

- Chromium etchant: Standard, Sigma Aldrich

- Developer: AZ 726 MIF Developer, Merck performance Materials GmbH

- EG: Ethylene glycol, $\geq 95\%$, Sigma Aldrich

- $[EMIM][EtSO4]$: (1-Ethyl-3-methylimidazolium ethyl sulfate), $\geq 95\%$, Sigma Aldrich

- Gold etchant: Standard, Sigma Aldrich HHPAA (2-Hydroxy-4'-(2-hydroxyethoxy)-2-methylpropiophenone), 98%, Sigma Aldrich

- MBBAm (N,N'-Methylenebisacrylamide), 99%, Sigma Aldrich

- NIPAm: (N-Isopropylacrylamide), 97%, Alfa Aesar

- Orthogonal Developer: Orthogonal Developer 103a, Orthogonal Inc.

- Orthogonal Photoresist for undoped species: NLOF, Orthogonal Inc.

- Sacrificial layer: Sacrifical Layer (SL), Orthogonal Inc.

- Orthogonal Photoresist for doped species: OSCoR 4020 Photoresist, Orthogonal Inc.

- Orthogonal Stripper: Orthogonal Stripper 900, Orthogonal Inc.

- p(g3T2-T): 3-(2-(2-(2-methoxyethoxy)ethoxy)ethoxy)thiophene

- Dopants: 1,3,4,5,7,8-hexafluorotetracyanonaphthoquinodimethane and 1,3,4,5-tetrafluorotetracyanonaphthoquinodimethane

- Photoresist: AZ 1518 Photoresist, Merck Performance Materials GmbH & Microchemical GmbH

- Silane A174 (3-(Trimethoxysilyl)propyl methacrylate), TCI

3.2   Equipmment

- Baking: All baking steps were carried out on a Stuart SD160 digital hotplate (Stuart Equipment, UK).

- Electrical characterisation (ambient): Device characterisation under ambient conditions was performed on a Everbeing C-6 Probe Station (Everbeing Int'l Corp., Taiwan), connected to a Keithley 4200-SCS Semiconductor Characterisation System (Keithley Instruments, USA).

- Electrical characterisation (glovebox): Device characterisation was performed in a nitrogen-filled glovebox. Probing needles were connected to two Keithley 236 Source Measure Units (Keithley Instruments, USA).

- Impedance measurements: Impedance measurements were carried out by using a Metrohm Autolab PGSTAT302N potentiostat/galvanostat (Metrohm AG, Switzerland).

- Micrographs: Micrographs were taken on a Nikon Eclipse LV100ND microscope, equipped with a DS-Fi2 camera (Nikon, Japan).

- Photolithography: Photolithography was carried out on a SÜSS Microtec MJB4 maskaligner system (SÜSS Microtec AG, Germany).

- Photomasks: Photomasks were custom made by Compugraphics Jena in a 4 inch format (soda-lime glass covered with chromium) and held several mask designs (Compugraphics Jena GmbH, Germany).

- Plasma cleaning: O2-plasma cleaning was performed by using a Harrick PDC-002 plasma cleaner (Harrick Plasma, USA), connected to a Leybold Heraeus Combitron CM 330 Vacuum Gauge Controller (Leybold GmbH, Germany).

- Plasma etching. O2-plasma etching was performed by using a Diener electronic ATTO plasma cleaner (Diener electronic GmbH & Co. KG, Germany).

- Profilometry. Profilometry was performed on a Veeco Dektak 150 surface profiler (Veeco Instruments Inc., USA).

- UV-Visible Spectroscopy: SolidSpec-3700 UV-Vis-NIR spectrometer from Shimadzu.

- Ultraviolet Photoelectron Spectroscopy (UPS): a helium discharge lamp (UVS10/35, Specs) was used and the main He I excitation line is at hv = 21.22 eV

- Spincoating. Samples were coated with a SAWATEC SM-180-BT spincoater (SAWATEC AG, Switzerland).

3.3   Software

- Data processing: All data was processed by customised scripts written in the Python programming language. Mathematical computations (e.g. fits, integration) were carried out by employing the Pandas, NumPy, and SciPy libraries. Visualisations were performed using the Matplotlib library.

- Electrical characterisation: Electrical characterisations were performed by controlling SMUs through the in-house developed SweepMe! software ().

- Profilometry: Profilometry was performed by using the Dektak software (Veeco Instruments Inc., USA).

3.4   Photomasks

Photomasks were employed during photolithography to cover or uncover the respective areas of interest, depending on the photoresist employed (positive or negative, respectively). Details are given in Chapter . The employed photomasks for OECT fabrication are shown in Figure , with a labeled close-up scheme of a transistor device given in Figure . All devices were designed in a side-gate structure with the 16 devices each mask comprised differing in channel length and gate distance. An overview of the specific dimensions is provided in Table with the designations assigning the devices (U1 – U8 (Up) and D1 – D8 (Down)). Since investigations on device dimensions were not a direct study object of this work, according assignments were left out. However, all comparisons between different substrates do of course always refer to the very same devices on each individual sample. A device assignment of all plots shown is given in Table S1. It shall be pointed out that the fabrication process did regularly lead to samples with several non-functioning devices. Accordingly, experiments were to be conducted on OECTs that were found working, which accounts for the variation in examined devices. For experiments of Chapter , available photomasks were arranged and covered to yield the setup shown in Figure . For experiments of Chapter , channels of p(g3T2-T) with underlying gold contacts were prepared. The corresponding photomasks are shown in Figure and were printed on plastic foil in a common inkjet printer. As schematically shown in Figure though, the lower big as well as several small gold contacts have not been used during execution. The lowest small gold contact served as source electrode.

3.5   Experimental Procedures

3.5.1   Conjugated polymer films

Unlike in reference [3], where drop cast is used to fabricate devices, in order to perform lithography and being able to do a miniaturization process, homogeneous films are needed. The following procedure has been stablished:

1. prepare 10mg/mL solution of p(g3T2-T) in chloroform at 60°C,

2. prepare 5, 10 and 20 mg/mL solution of F_4TCNQ in acetonitrile at 60°C,

3. clean substrates with subsequent steps of ultrasonic bath with acetone for 15 minutes, rinse cith IPA, drying with N_2 and O_2-plasma,

4. dynamic spin coat $70\mu L$ of p(g3T2-T) at 3000RPM for 60s,

5. if preparing a doped sample, dynamic spin coat $140\mu L$ of each dopant solvent at different concentrations on top, to yield approximately 70 nm thick layer, and

6. postbake at 80°C.

3.5.2   Fabrication of Organic Electrochemical Transistors

After following the patterning process to obtain Au contacts from reference , undoped and doped p(g3T2-T) was deposited following the procedure described before. After some trials, different patterning process were defined for undoped and doped films.

3.5.2.1   Undoped p(g3T2-T) OECT

1. Sacrificial Layer 1 (SL1, fluoropolymer provided by Orthogonal Inc.) was spincoated (6000 RPM for 60s) and baked for 60s at 113°C.

2. To promote adhesion, sample was placed in plasma (UFO2) for 60s.

3. NLOF 2020 (commercial negative-tone photoresist from Microchemicals) was spincoated (3000 RPM for 60s) and baked for 60s at 113°C.

4. NLOF was exposed for 12s to structure channel and gate (although only channel is used).

5. After postbaking (60s at 113°C), NLOF was developed by rinsing the sample in AZ MIF 726 (commercial developer for NLOF 2020) for 20s and wash off in DI water (carried out extra times if necessary).

6. SL1 was developed using HF 7300 developer for 20s and spin rinsed at 3000RPM (carried out extra times if necessary):

7. Excess p(g3T2-T) was removed by O_2-plasma etching (180s)

8. Finally, the sample was placed in Orthogonal Stripper 902 overnight at room temperature.

9. Ultrasonic bath with stripper is followed if NLOF pattern is still on sample.

3.5.2.2 Doped p(g3T2-T) OECT

1. Orthogonal photoresist OSCoR 4020 (provided by Orthogonal Inc.) was spin-coated (3000 RPM for 60s) and baked for 60s at 103°C.

2. OSCoR was exposed for 20s (increase one extra cycle if using higher dopant concentration) to structure channel and gate (although only channel is used).

3. After postbaking (60s at 103°C), development followed by covering the sample with Ortoghonal Developer 103a and removing it by spinning at 3000RPM after 50s (carried out extra times if necessary, if higher dopant concentration is used, start with 30s development).

4. Excess doped p(g3T2-T) was removed by O_2-plasma etching (180s)

5. The sample was placed in Orthogonal Stripper 902 over night at room temperature.

6. Finally, to prepare for measurements, blow off excess of stripper with N_2 and add $20\mu L$ of solid state electrolyte (SSE) in liquid state.

Chapter 4

Results and Discussion

4.1 Doped Conjugated Polymer films

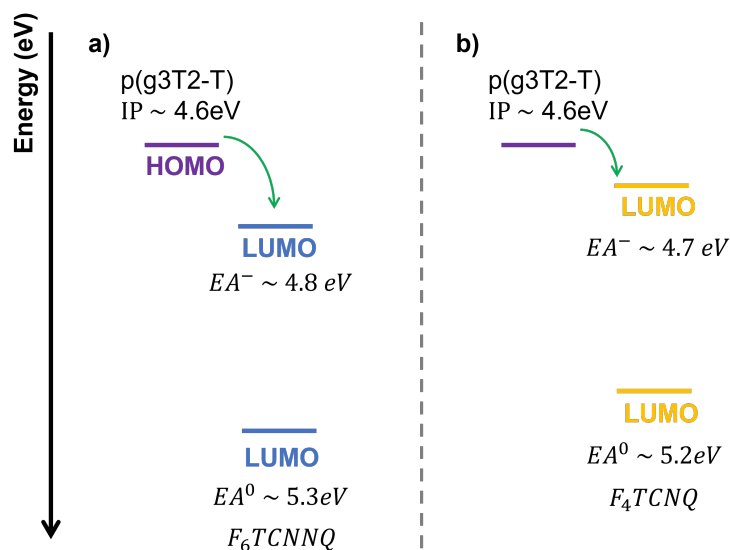As followed in the procedure part...

FIGURE 4.1: Energy diagram of p(g3T2-T) with a) F_6TCNNQ and b) F_4TCNNQ. Ionization potential of p(g3T2-T) extracted from reference [3] and electron affinities of the neutral species (EA^0) and of the anion (EA^-) of the dopants are extracted from cyclic voltammetry measurements in reference [8].

4.1.1 Polaron and Bipolar formation

4.1.2 Workfunction increase

4.1.3 Redox properties with Solid State Electrolyte Precursor

4.2 Organic Electrochemical Transistors

4.2.1 Channel and gate morphology

4.2.2 Channel conductivity

Prior biasing gate, which is due to passive (ion) diffusion?

4.2.2.1 Under inert conditions

4.2.2.2 Under ambient conditions

4.2.3 Threshold voltage shift

The fact that solution-sequential doped films allows better homogeneity [10], make it also more compatible with microstructuring processes such as photolithography. At the expense of enabling easier and more precise control of doping levels [11].

The Ag/AgCl gate electrode's work function is reasonably constant, the work function of an OMIEC gate electrode however may vary depending on its processing history and redox reactions with other species present in the electrolyte (e.g. molecular oxygen).28 Applying VGS only determines the potential difference between the gate and channel but does not control the potentials of either electrode (hence the position of the Fermi level) with respect to a reference. This leads to many challenges in operating an OECT with OMIEC gate electrodes.

4.2.4 Important figures of merit

Chapter 5

Conclusion and Outlook

Bibliography

[1] J. Rivnay, S. Inal, A. Salleo, R. M. Owens, M. Berggren, and G. G. Malliaras, "Organic electrochemical transistors," *Nature Reviews Materials*, vol. 3, no. 2, pp. 1–14, 2018.

[2] C. B. Nielsen, A. Giovannitti, D.-T. Sbircea, E. Bandiello, M. R. Niazi, D. A. Hanifi, M. Sessolo, A. Amassian, G. G. Malliaras, J. Rivnay, and I. McCulloch, "Molecular Design of Semiconducting Polymers for High-Performance Organic Electrochemical Transistors," *Journal of the American Chemical Society*, vol. 138, no. 32, pp. 10 252–10 259, 2016.

[3] S. T. M. Tan, G. Lee, I. Denti, G. LeCroy, K. Rozylowicz, A. Marks, S. Griggs, I. McCulloch, A. Giovannitti, and A. Salleo, "Tuning Organic Electrochemical Transistor Threshold Voltage using Chemically Doped Polymer Gates," *Advanced Materials*, vol. 34, no. 33, p. 2202359, 2022.

[4] A. Weissbach, L. M. Bongartz, M. Cucchi, H. Tseng, K. Leo, and H. Kleemann, "Photopatternable solid electrolyte for integrable organic electrochemical transistors: Operation and hysteresis," *Journal of Materials Chemistry C*, vol. 10, no. 7, pp. 2656–2662, 2022.

[5] B. Lüssem, M. Riede, and K. Leo, "Doping of organic semiconductors," *physica status solidi (a)*, vol. 210, no. 1, pp. 9–43, 2013.

[6] B. D. Paulsen, K. Tybrandt, E. Stavrinidou, and J. Rivnay, "Organic mixed ionic–electronic conductors," *Nature Materials*, vol. 19, no. 1, pp. 13–26, Jan. 2020.

[7] D. A. Bernards and G. G. Malliaras, "Steady-State and Transient Behavior of Organic Electrochemical Transistors," *Advanced Functional Materials*, vol. 17, no. 17, pp. 3538–3544, 2007.

[8] D. Kiefer, R. Kroon, A. I. Hofmann, H. Sun, X. Liu, A. Giovannitti, D. Stegerer, A. Cano, J. Hynynen, L. Yu, Y. Zhang, D. Nai, T. F. Harrelson, M. Sommer, A. J. Moulé, M. Kemerink, S. R. Marder, I. McCulloch, M. Fahlman, S. Fabiano, and C. Müller, "Double doping of conjugated polymers with monomer molecular dopants," *Nature Materials*, vol. 18, no. 2, pp. 149–155, Feb. 2019.

[9] M. L. Tietze, L. Burtone, M. Riede, B. Lüssem, and K. Leo, "Fermi level shift and doping efficiency in p-doped small molecule organic semiconductors: A photoelectron spectroscopy and theoretical study," *Physical Review B*, vol. 86, no. 3, p. 035320, Jul. 2012.

[10] I. E. Jacobs, E. W. Aasen, J. L. Oliveira, T. N. Fonseca, J. D. Roehling, J. Li, G. Zhang, M. P. Augustine, M. Mascal, and A. J. Moulé, "Comparison of solution-mixed and sequentially processed P3HT:F4TCNQ films: Effect of doping-induced aggregation on film morphology," *Journal of Materials Chemistry C*, vol. 4, no. 16, pp. 3454–3466, Apr. 2016.

[11] S. T. M. Tan, "Organic Mixed Ionic Electronic Conductors for Electrochemical Devices," Ph.D. dissertation, Stanford University, Palo Alto, CA, Dec. 2022.

[12] G. A. Snook, P. Kao, and A. S. Best, "Conducting-polymer-based supercapacitor devices and electrodes," *Journal of Power Sources*, vol. 196, no. 1, pp. 1–12, Jan. 2011.

[13] Y. Liang, Z. Tao, and J. Chen, "Organic Electrode Materials for Rechargeable Lithium Batteries," *Advanced Energy Materials*, vol. 2, no. 7, pp. 742–769, 2012.

[14] A. Giovannitti, R. B. Rashid, Q. Thiburce, B. D. Paulsen, C. Cendra, K. Thorley, D. Moia, J. T. Mefford, D. Hanifi, D. Weiyuan, M. Moser, A. Salleo, J. Nelson, I. McCulloch, and J. Rivnay, "Energetic Control of Redox-Active Polymers toward Safe Organic Bioelectronic Materials," *Advanced Materials*, vol. 32, no. 16, p. 1908047, 2020.

[15] S. T. M. Tan, A. Gumyusenge, T. J. Quill, G. S. LeCroy, G. E. Bonacchini, I. Denti, and A. Salleo, "Mixed Ionic–Electronic Conduction, a Multifunctional Property in Organic Conductors," *Advanced Materials*, vol. 34, no. 21, p. 2110406, 2022.

[16] J. T. Friedlein, R. R. McLeod, and J. Rivnay, "Device physics of organic electrochemical transistors," *Organic Electronics*, vol. 63, pp. 398–414, Dec. 2018.

[17] D. Moia, A. Giovannitti, A. A. Szumska, I. P. Maria, E. Rezasoltani, M. Sachs, M. Schnurr, P. R. F. Barnes, I. McCulloch, and J. Nelson, "Design and evaluation of conjugated polymers with polar side chains as electrode materials for electrochemical energy storage in aqueous electrolytes," *Energy & Environmental Science*, vol. 12, no. 4, pp. 1349–1357, 2019.

[18] M. Moser, L. R. Savagian, A. Savva, M. Matta, J. F. Ponder, T. C. Hidalgo, D. Ohayon, R. Hallani, M. Reisjalali, A. Troisi, A. Wadsworth, J. R. Reynolds, S. Inal, and I. McCulloch, "Ethylene Glycol-Based Side Chain Length Engineering in Polythiophenes and its Impact on Organic Electrochemical Transistor Performance," *Chemistry of Materials*, vol. 32, no. 15, pp. 6618–6628, 2020.

[19] S. Inal, G. G. Malliaras, and J. Rivnay, "Benchmarking organic mixed conductors for transistors," *Nature Communications*, vol. 8, no. 1, p. 1767, Nov. 2017.

[20] S. T. Keene, T. P. A. van der Pol, D. Zakhidov, C. H. L. Weijtens, R. A. J. Janssen, A. Salleo, and Y. van de Burgt, "Enhancement-Mode PEDOT:PSS Organic Electrochemical Transistors Using Molecular De-Doping," *Advanced Materials*, vol. 32, no. 19, p. 2000270, 2020.

[21] A. Savva, C. Cendra, A. Giugni, B. Torre, J. Surgailis, D. Ohayon, A. Giovannitti, I. McCulloch, E. Di Fabrizio, A. Salleo, J. Rivnay, and S. Inal, "Influence of Water on the Performance of Organic Electrochemical Transistors," *Chemistry of Materials*, vol. 31, no. 3, pp. 927–937, Feb. 2019.